

**1 SCAN10: A REPRODUCIBLE AND STANDARDIZED**  
**2 PIPELINE FOR PROCESSING 10X SINGLE CELL RNASEQ**  
**3 DATA**

**4** Maxime Lepetit<sup>1</sup>, Mirela Diana Ilie<sup>2,3</sup>, Marie Chanal<sup>2</sup>, Gerald Raverot<sup>2,4</sup>,  
**5** Philippe Bertolino<sup>2</sup>, Franck Picard<sup>1</sup> and Olivier Gandrillon<sup>1,5,\*</sup>.

**6** 1 - ENS de Lyon, CNRS UMR 5239, Laboratory of Biology and Modelling  
**7** of the Cell, Lyon, France.

**8** 2 - Centre de Recherche en Cancérologie (CRCL) - INSERM 1052 - CNRS  
**9** 5286 - Centre Léon Bérard - Université Claude Bernard Lyon 1, Institut  
**10** Convergence Plascan, Lyon, France.

**11** 3 - Endocrinology Department, "C.I.Parhon" National Institute of Endocrinol-  
**12** ogy, Bucharest, Romania.

**13** 4 - Endocrinology Department, Reference Center for Rare Pituitary Diseases  
**14** HYPO, Groupement Hospitalier Est" Hospices Civils de Lyon, Bron, France.  
**15** 5 - Inria Center Grenoble Rhone-Alpes, Equipe Dracula, Villeurbanne, France.

**16** Keywords : pipeline, single cell transcriptomics, data analysis, mapping,  
**17** annotation

## <sup>18</sup> 1 Abstract

<sup>19</sup> The recent explosion of single cell transcriptomics has led to the challenge of  
<sup>20</sup> developing data analysis pipelines that are both fully reproducible and mod-  
<sup>21</sup> ular while allowing interoperability across multiple systems and institutions.  
  
<sup>22</sup> We present scAN10, a processing pipeline of 10X single cell RNAseq data,  
<sup>23</sup> that inherits the ability to be executed on most computational infrastruc-  
<sup>24</sup> tures, thanks to Nextflow DSL2. The modular nature of Nextflow pipelines  
<sup>25</sup> allows to easily integrate and assess different blocks for a given analysis step.  
  
<sup>26</sup> We illustrate the benefit of using scAN10 by showing its ability to assess  
<sup>27</sup> the impact of the mapping step on the resulting output using a clinical 10X  
<sup>28</sup> scRNAseq analysis of a human pituitary gonadotroph tumour.

## <sup>29</sup> 2 Introduction

<sup>30</sup> The recent explosion of single cell transcriptomics, mostly through scR-  
<sup>31</sup> NAseq, has led to the challenge of developing data analysis pipelines that are  
<sup>32</sup> both fully reproducible and modular while allowing interoperability across  
<sup>33</sup> multiple systems and institutions.

<sup>34</sup> The initial step in scRNAseq data analysis consist in generating a count  
<sup>35</sup> matrix from **fastq** sequence files. This step is often overlooked (see e.g. [1]),  
<sup>36</sup> although it can represent a very critical step (see e.g. [2]). Therefore one  
<sup>37</sup> needs freely available analysis pipeline that could allow to verify the impact  
<sup>38</sup> of some early analysis step easily, such as the nature of the GTF file used [3]  
<sup>39</sup> or downstream steps such as the normalization method on the generation of  
<sup>40</sup> the count matrix.

<sup>41</sup> The most widely used existing solutions like the Seurat suite [4] have been  
<sup>42</sup> designed to be as much user-friendly as possible and therefore does not offer  
<sup>43</sup> easy solution for incorporating alternative low-level analysis steps.

<sup>44</sup> This is why in the present paper we approached this challenge by designing  
<sup>45</sup> **scAN10**, a processing pipeline of 10X single cell RNAseq data, that inherits  
<sup>46</sup> the ability to be executed on most computational infrastructures, thanks to  
<sup>47</sup> Nextflow DSL2. The modular nature of Nextflow pipelines allows to easily  
<sup>48</sup> integrate and assess different bricks blocks for a given analysis step. **scAN10**  
<sup>49</sup> is available as an open source Gitlab repository. It takes raw paired-end

50 `fastq` files and genomic files (FASTA and GTF annotation files) as input,

51 and outputs a clustered dimensionally-reduced version of the dataset.

52 We illustrate the benefit of using `scAN10` by showing its ability to assess the

53 impact of the mapping step on the resulting UMAP projection as well as on

54 some specific gene identification using a clinical 10X scRNA-seq analysis of

55 one human pituitary gonadotroph tumour.

## 56 3 Results

### 57 3.1 Pipeline description

58 Figure 1 describes the overall processing of the sequencing files with the

59 ordering of all steps described in section 5.

### 60 3.2 Raw dataset

61 To showcase the applicability of `scAN10` we processed a clinical dataset from

62 a human pituitary gonadotroph tumour acquired from one male patient and

63 sequenced by 10Xgenomics. The dataset was processed using `scAN10` with

64 the following parameters :

65 • `max_feature_RNA = 7000`

66 • `max_percent_mito= 25`

67 The clustering (resolution =0.7) and UMAP embedding were done based on

68 the ten first principal components of the PCA, as determined by the rule of  
69 thumb heuristic and the broken stick method [5].

70 **3.3 Version annotation effect**

71 We first assess the impact of the Ensembl version of the GTF file on the final  
72 output. GTF files and their corresponding FASTA files were downloaded via  
73 `ftp` protocol using the `--version` parameter (see section 5). We set Cellranger  
74 as the default mapper and then assessed the impact of 4 different annotation  
75 releases (93, 98, 103 and 106) on the number of detected genes (figure 2A)  
76 and on the count per genes as assessed with the CHGA gene. (Figure 2B).

77 The overall impact of the GTF version seems relatively modest, especially in  
78 regard to the number of counts. The 106 version allowed to identify a larger  
79 number of genes and was kept for the next step.

80 **3.4 Comparing filtered with unfiltered annotations**

81 We then assessed the impact of filtrating the GTF file with the `mkgtf` Cell-  
82 ranger function. This filtration step is intended to remove unwanted genes  
83 classified by biotype. We used the default values of that function that re-  
84 moves biotypes such as `gene.biotype:pseudogene` from the GTF annotation  
85 file.

86 This step removes some ambiguity between reads location by allowing reads  
87 that would be flagged as multi mapped reads to be included in the quantifi-

88 cation.

89 We observed that this filtration step indeed had a major impact on both the  
90 number of genes detected (Figure 3A) but also on gene counts (Figure 3B).

### 91 **3.5 Cellranger versus Kallisto-bustools**

92 We then compared the impact of two popular alignment tools for single-cell  
93 RNA sequencing (Kallisto-bustools and Cellranger) using the 10x Genomics  
94 pre-built Cellranger reference packages version 2020-A for human.

95 As seen in Figure 4A, 81 % of the genes were identified by both algorithms  
96 whereas Kallisto-bustools identified more genes than Cellranger.

97 The impact of the mapper on counts for specific genes seemed to be negligible  
98 (Figure 4B). Therefore this tends to favor Kallisto-bustools for downstream  
99 analyses.

100 We finally assessed the impact of the mapper choice on the final clustering  
101 step. As seen in Figure 5, the impact was modest but apparent (e.g. cluster  
102 number 1 in the CR dataset was split in two in the KB dataset).

## 103 **4 Discussion**

104 We described **scAN10**, a Nextflow based processing pipeline of 10X single cell  
105 RNAseq data.

106 By applying **scAN10** to a clinical dataset we showed that the impact of the  
107 annotation version was relatively modest although using the latest Ensembl  
108 release (106) of the GTF and FASTA allows to identify a larger number of genes.

109 As expected, filtrating the GTF files by removing unwanted genes based on  
110 10X reference packages generation had a major impact both on the number  
111 of genes but also on gene counts.

112 However, recent study observed differences in the mitochondrial content of  
113 the resulting cells when comparing a filtered annotation to the full annota-  
114 tion. Therefore removing processed pseudogene might lead to an enrichment  
115 of the mitochondrial content [6].

116 Furthermore when using Kallisto-bustools instead of Cellranger the impact  
117 of the count numbers for specific genes seemed to be small but meaningful.  
118 Kallisto-bustools produced higher total number of genes detected which 5169  
119 unique genes as compared to Cellranger.

120 The final combination that was found to be the most effective for our dataset  
121 therefore was using Kallisto-bustools together with the filtered version of  
122 the 106 GTF. There is no reason to believe that such parameters might be  
123 universally applicable, and we therefore recommend the use of **scAN10** so  
124 assess such an impact on any other dataset before proceeding with higher  
125 level analysis.

126 With Nextflow each step is encapsulated in independent blocks called pro-

127 cesses. Each process communicates via channels. The orchestration of the  
128 workflow with DSL2 syntax allows to easily modify the pipeline, by adding  
129 new processes modules. In the future we expect to include some normaliza-  
130 tion procedures to the pipeline:

131 • The basic global-scaling normalization method from Seurat that di-  
132 vides the feature expression for each cell by the total expression and  
133 multiplies this by a scale factor and log-transforms the result.[7]

134 • **Sctransform** which uses regularized negative binomial regression and  
135 computes Pearson residuals that correspond to the normalized expres-  
136 sion levels for each transcript.[8]

137 • **Scran** which uses pooling-based size factor estimation.[9]

138 The use of **scAN10** should be made straightforward to assess a combination of  
139 low-level steps together with the normalization step on the resulting output.

140 One major limitation using Nextflow is a lack of interactivity during pipeline  
141 running. Indeed, when Nextflow pipelines run, although it can output files,  
142 there is no interactive dialogue that could allow the user to modify parameters  
143 during the run. All the pipelines parameter need to be defined and set in the  
144 launching command.

145 We finally believe that **scAN10** will be a useful tool for the growing community  
146 of 10X scRNAseq *aficionados*.

## <sup>147</sup> 5 Material and methods

### <sup>148</sup> 5.1 Study ethic approval

<sup>149</sup> This work is part of the SPACE-PIT study (MR004 n21-5439). It was ap-  
<sup>150</sup> proved by the Hospices Civils de Lyon ethical committee and registered at  
<sup>151</sup> the “Centre National Information et Liberté” ( [CNIL.fr](http://CNIL.fr) ) under the reference  
<sup>152</sup> 20\_098. Informed consent was obtained from the patient.

### <sup>153</sup> 5.2 Single cells preparation and sequencing

<sup>154</sup> A tumor fragment from a gonadotroph surgically-resected adenoma was col-  
<sup>155</sup> lected in Dulbecco’s Modified Eagle Medium (DMEM, cat 41965062; Life  
<sup>156</sup> Technologies). Single-cell suspension of the resected fragment was obtained  
<sup>157</sup> through mechanical enzymatic dissociation (Collagenase P, cat 11213865001)  
<sup>158</sup> then passed through a 100  $\mu$ m mesh-strainer (#732-2759, VWR interna-  
<sup>159</sup> tional).

<sup>160</sup> Red blood cells were eliminated using a 10-minute incubation with a com-  
<sup>161</sup> mercial red blood cell lysis buffer (eBioscience, cat #00-4300-54). The whole  
<sup>162</sup> process was achieved within the 2 hours following the surgical resection,  
<sup>163</sup> cell viability was evaluated to reach at least 70 percent prior encapsula-  
<sup>164</sup> tion. Generation of the library was done using a Chromium controller from  
<sup>165</sup> 10xGenomics. The entire procedure was achieved as recommended by the  
<sup>166</sup> manufacturer’s for the v3 reagent kit (10xGenomics). Single cell suspension

167 was loaded onto a Chromium Single Cell A Chip, aiming for 5,000 cells. The  
168 cDNA was amplified after a reverse transcription step prior a SPRIselect  
169 (Beckman Coulter), a cleaning, a quantification and an enzymatic fragmen-  
170 tation prior to the library sequencing on a NextSeq500 system (Illumina).

### 171 **5.3 Implementation**

172 The **scAN10** pipeline was powered and supported by the reactive workflow  
173 manager Nextflow [10]. In addition, the pipeline was coded with the DSL2  
174 syntax extension. Nextflow simplifies the writing of computational pipelines  
175 by making them portable, scalable,parallelizable and ensuring a high level of  
176 reproducibility. Nextflow provides native support for container technologies  
177 such as Docker or Singularity. Each process in the pipeline will be run in  
178 a container. A reproducible container environment is built for each process  
179 from Docker images stored on the DockerHub. The analyses can be run  
180 on the user's preferred computing platform. Using the configuration file and  
181 corresponding profile, the pipeline can be run on a local computer via Docker  
182 or Singularity, as well as on a high-performance computing (HPC) cluster  
183 or in cloud-based environments. Nextflow includes a cache-based pipeline  
184 resume feature, no matter what the reason was for its stopping.

185 **5.4 Input**

186 **scAN10** takes three mandatory parameters as input: the paired-end FASTQ R1  
187 and R2 from 10X Chromium sequencing and two genomics files (one FASTA  
188 an one GTF).

189 FASTQ files store the nucleotide sequence and the associated sequencing qual-  
190 ity scores. Those files must be provided through the `--fastq` pipeline pa-  
191 rameter and needs to be compressed in `gzip` format. Reads are sequenced  
192 in paired-ends thus 2 reads will be produced for each sequencing lane. In  
193 the case a sample has been sequenced on several lanes, all reads R1 can be  
194 concatenate together and all reads R2 together. The mapping step require  
195 the input of two additional files corresponding to the species of interest:

196 

- 197 • A `FASTA` genomic file which stores the raw genome sequence.
- 198 • A Gene transfer format (`GTF`) file which stores genome annotation in-  
cluding gene positions.

199

200 One should note that for human datasets, `FASTA` and `GTF` files can be down-  
201 loaded automatically by specifying a version number as an entry parameter  
202 (`--version`) available on the ENSEMBL database.

## 203 5.5 Preprocessing & Mapping

204 First, FASTQ files are processed and trimmed by using `Fastp` v0.20.1 , an  
205 ultra-fast FASTQ preprocessor with useful quality control and data-filtering  
206 features [11]. Reads with phred quality  $\geq 30$  (-q 30) is qualified to the quan-  
207 tification step. Length filtering is disabled (-L) while adapter sequence auto-  
208 detection is enabled (--detect\_adapter\_for\_pe).

209 To reduce overlapping annotation, we recommend and provide an optional  
210 parameter --filtergtf allow the GTF filtration with Cellranger's `mkgtf` function  
211 based on the same biotype attribute used to generate the GTF file for the hu-  
212 man Cell Ranger reference package. (see : <https://support.10xgenomics.com/single-cell-gene-expression/software/release-notes/build> )

214 The processed files are then mapped of a reference genome to quantify gene  
215 expression. In `scAN10`, the user can specify two different mappers (see below):  
216 Kallisto-bustools v0.26.0 [12] or Cellranger v5.0.1 [13].

217 • Kallisto-bustools is used thought the Python wrapper : `kb_python`.  
218 Starting with FASTA and GTF files an index of the reference can be built  
219 as a colored De Bruij graph with Kallisto via `kb ref`. with default pa-  
220 rameter. Once an index has been generated or downloaded, `kb count`  
221 uses Kallisto to pseudoalign reads and `bustools` to quantify the data.

222 • Cellranger created and prepared reference package with Cellranger's  
223 `mkref` function. The alignment was run via Cellranger's `count` with

224 default parameters as described on `10xgenomics.com`.

## 225 5.6 Quality control

226 **Empty Droplets** With Droplet-based data most of the barcodes in the  
227 matrix correspond to empty droplets (eg barcode with sum expression over  
228 gene of 0). While Cellranger takes care of the empty droplet filtering, empty  
229 droplets from Kallisto-bustools gene expression matrix need to be removed.  
230 The Kallisto-bustools outputs were imported into R with customed R func-  
231 tion. The UMI total counts were ranked using `DropletUtils::barcodeRanks`  
232 function from `DropletUtils` v1.14.2 . Empty droplets were removed by se-  
233 lecting the inflection point value on the resulting knee plot (lower cutoff =  
234 10). The Cellranger matrix is imported from the standard filtered barcode  
235 output. After importation, either gene expression matrices were converted as  
236 Seurat object (Seurat v4.0.4) with `Seurat::CreateSeuratObject` function,  
237 including features detected in at least 3 cells (min.cells =3).

238 **Low quality cells** After removing empty droplets the pipeline computes 3  
239 QC metrics per sample: the number of unique features per cells, the number  
240 of UMIs by cells and the percent of mitochondrial counts by cells. These QC  
241 metrics are then used to discard three main types of low quality cells [14] :

242 1. Cells in apoptosis may exhibit high % mitochondrial and low number  
243 of UMIs per cells

244        2. Cells that failed during library preparation exhibit low number of unique  
245            gene counts and low number of UMIs per cells

246        3. The pipeline uses the R package `DoubletFinder` v2.0.3 to detect and  
247            remove the potential doublets from the dataset. See [15] and [16].

248        **Thresolding** Default thresholding parameters used by the `scAN10` pipeline  
249            are:

250        1. `min_feature_RNA=500`

251        2. `min_ncount_RNA=0`

252        3. `max_percent_mito="adaptive"`

253        4. `max_feature_RNA="adaptive"`

254        5. `max_ncount_RNA="adaptive"`

To define maximum values of threshold `scAN10` allows to use an adaptive filter defined by a certain number of median absolute deviations (MADs) away from the median [17]:

$$\text{median} + 3 * \text{mad}$$

255        **Non-expressed genes** Genes with sum count along cells equal to 0 (eg  
256            not-expressed genes) are removed.

## 257 5.7 Normalization

258 To normalize the filtered gene expression matrix, the user can use **Sanity**,  
259 a Bayesian algorithm to infer gene-expression state [18]. We are fully aware  
260 that the normalization of single cell transcriptomic data is a research field on  
261 its own (see e.g. [2] and citations therein), and we expect this block in the  
262 pipeline to be susceptible to be modified in future versions of the pipeline.  
263 The modularity of the Nextflow syntax makes it ideal for such additions.

## 264 5.8 Clustering and two-dimensional visualization

265 A final step consists in variable features selection with **Seurat**::**FindVariableFeatures**  
266 using the **vst** method (selection.method = "vst") and selecting the 2000 first  
267 highly variable genes (nfeatures = 2000), followed by a first linear dimension-  
268 ality reduction using PCA (Seurat::RunPCA with default parameter). The  
269 M first axis of the PCA are then used for the nearest-neighbor graph con-  
270 struction with **Seurat**::**FindNeighbors** function (dims=1:M).

271 Cluster determination was performed using the Louvain algorithm [19] run  
272 with **Seurat**::**FindClusters** function (algorithm = 1). The resolution pa-  
273 rameter set by default to 0.7 is use for increasing (values >1) or decreasing  
274 (values <1) the number of clusters obtained. The quality of the clustering  
275 was assessed using the Silhouette score [20]. Finally, non-linear dimensional  
276 representation (using either t-SNE [21] or UMAP [22]) is then performed  
277 using **Seurat**::**RunTSNE** or **Seurat**::**RunUMAP** with default parameters using

278 the same number of dimensions than the nearest-neighbor graph building.

279 The resolution parameters used for clustering and the number of principal  
280 components kept for both clustering and dimension reduction embeddings  
281 can be respectively modified by the user at the start of the pipeline by the  
282 `--resolution_clustering` and the `--principal_component` parameters.

283 Alternatively this last step can be skipped allowing the user to use their own  
284 clustering method. Similarly, to avoid the introduction of layers of complexity  
285 and simplify the pipeline usage, the automatic annotation of clusters was not  
286 introduced. Users can annotate their dataset manually.

## 287 **5.9 Output**

288 Exhaustive list of processes outputs is available on the Readme of the gitlab  
289 repository (section 6).

## 290 **6 Availability**

291 scAN10 is freely available at : <https://gitbio.ens-lyon.fr/LBMC/sbdm/>  
292 `scan10`

## 293 **7 Acknowledgements**

294 We thank the Institut Convergence Plascan (Grant Number ANR-17-CONV-  
295 0002) for their support.

296 Mirela Diana Ilie has been supported by the Fondation ARC pour la recherche  
297 sur le cancer (ARCMD-DOC12020020001361).

298 We thank (i) Emmanuel Jouanneau and Alexandre Vasiljevic from the Neu-  
299 rosurgery and Pathology Departments, Reference Center for Rare Pituitary  
300 Diseases HYPO, “Groupement Hospitalier Est ”Hospices Civils de Lyon,  
301 Bron, France for providing diagnosed Gonadotroph tumor material; (ii) Hec-  
302 tor Hernandez-Vargas for his advices and support with setting the single cell  
303 dissociation and subsequent bioinformatic analysis; and (iii) Laurent Modolo  
304 from the LBMC for his help using the Nextflow syntax.

305 We thank the Pôle Scientifique de Modélisation Numérique (PSMN, Ecole  
306 Normale Supérieure de Lyon) where computations were performed.

307 We finally thank the BioSyL Federation (<http://www.biosyl.org>), the LabEx  
308 Ecofect (ANR-11-LABX-0048) and the LabEx Milyon of the University of  
309 Lyon for inspiring scientific events.

## 310 8 Author contributions

311 Maxime Lepetit wrote the scAN10 script, performed the analysis, generated  
312 the figures and wrote the paper. Mirela Diana Ilie participated in generating  
313 and analyzing the 10X data. Marie Chanal participated in generating the  
314 10X data. Gerald Raverot participated in generating and analyzing the 10X  
315 data. Philippe Bertolino helped designing the study, analyzing the results,

316 reviewed and edited the manuscript, and secured the funding. Franck Picard  
317 helped designing the study and analyzing the results, reviewed and edited the  
318 manuscript, and secured the funding. Olivier Gandrillon helped designing the  
319 study and analyzing the results, wrote the paper, and secured the funding.

320 **9 References**

321 [1] M. D. Luecken and F. J. Theis. “Current best practices in single-cell  
322 RNA-seq analysis: a tutorial”. In: Mol Syst Biol 15.6 (2019), e8746.

323 [2] R. Zhang, G. S. Atwal, and W. K. Lim. “Noise regularization removes  
324 correlation artifacts in single-cell RNA-seq data preprocessing”. In:  
325 Patterns (N Y) 2.3 (2021), p. 100211.

326 [3] A.-H. Pool, H. Poldsam, S. Chen, M. Thomson, and Y. Oka. “En-  
327 hanced recovery of single-cell RNA-sequencing reads for missing gene  
328 expression data”. In: bioRxiv (2022), p. 2022.04.26.489449.

329 [4] Y. Hao, S. Hao, E. Andersen-Nissen, 3rd Mauck W. M., S. Zheng,  
330 A. Butler, M. J. Lee, A. J. Wilk, C. Darby, M. Zager, P. Hoffman,  
331 M. Stoeckius, E. Papalex, E. P. Mimitou, J. Jain, A. Srivastava, T.  
332 Stuart, L. M. Fleming, B. Yeung, A. J. Rogers, J. M. McElrath, C. A.  
333 Blish, R. Gottardo, P. Smibert, and R. Satija. “Integrated analysis of  
334 multimodal single-cell data”. In: Cell 184.13 (2021), 3573–3587 e29.

335 [5] D. A. Jackson. “Stopping Rules in Principal Components Analysis: A  
336 Comparison of Heuristical and Statistical Approaches”. In: Ecology 74  
337 (1993), pp. 2204–2214.

338 [6] Ralf Schulze Brüning, Lukas Tombor, Marcel H Schulz, Stefanie Dim-  
339 meler, and David John. “Comparative analysis of common alignment  
340 tools for single-cell RNA sequencing”. In: GigaScience 11 (Jan. 2022).  
341 giac001. eprint: [https://academic.oup.com/gigascience/article-  
342 pdf/doi/10.1093/gigascience/giac001/42297447/giac001.pdf](https://academic.oup.com/gigascience/article-pdf/doi/10.1093/gigascience/giac001/42297447/giac001.pdf).

343 [7] R. Satija, J. Farrell, and D. Gennert. “Spatial reconstruction of single-  
344 cell gene expression data.” In: Nat Biotechnol 33.5 (2015), pp. 495–  
345 502.

346 [8] C. Hafemeister and R. Satija. “Normalization and variance stabiliza-  
347 tion of single-cell RNA-seq data using regularized negative binomial  
348 regression.” In: Genome Biol 20.1 (2019), p. 296.

349 [9] A.T. L. Lun, K. Bach, and J.C. Marioni. “Pooling across cells to nor-  
350 malize single-cell RNA sequencing data with many zero counts.” In:  
351 Genome Biol 17.1 (2019), p. 75.

352 [10] P. Di Tommaso, M. Chatzou, E. W. Floden, P. P. Barja, E. Palumbo,  
353 and C Notredame. “Nextflow enables reproducible computational work-  
354 flows”. In: Nature biotechnology 35.4 (2017), pp. 316–319.

355 [11] S. Chen, Y. Zhou, Y. Chen, and J. Gu. “fastp: an ultra-fast all-in-one  
356 FASTQ preprocessor”. In: Bioinformatics 34.17 (2018), pp. i884–i890.

357 [12] P. Melsted, A. S. Booeshaghi, F. Gao, E. Beltrame, L. Lu, K. E.  
358 Hjorleifsson, J. Gehring, and L. Pachter. “Modular and efficient pre-  
359 processing of single-cell RNA-seq”. In: Nat. Biotechnol. 39 (2021), pp. 813–  
360 818.

361 [13] G. X. Zheng, J. M. Terry, P. Belgrader, P. Ryvkin, Z. W. Bent, R.  
362 Wilson, S. B. Ziraldo, T. D. Wheeler, G. P. McDermott, J. Zhu, M. T.  
363 Gregory, J. Shuga, L. Montesclaros, J. G. Underwood, D. A. Masque-  
364 lier, S. Y. Nishimura, M. Schnall-Levin, P. W. Wyatt, C. M. Hindson,  
365 R. Bharadwaj, A. Wong, K. D. Ness, L. W. Beppu, H. J. Deeg, C. Mc-  
366 Farland, K. R. Loeb, W. J. Valente, N. G. Ericson, E. A. Stevens, J. P.  
367 Radich, T. S. Mikkelsen, B. J. Hindson, and J. H. Bielas. “Massively  
368 parallel digital transcriptional profiling of single cells”. In: Nat Commun  
369 8 (2017), p. 14049.

370 [14] T. Ilicic, J.K. Kim, A.A. Kolodziejczyk, F.O. Bagger, D.J. McCarthy,  
371 J.C. Marioni, and Teichmann S.A. “Classification of low quality cells  
372 from single-cell RNA-seq data.” In: Genome Biology 17.1 (2016), p. 29.

373 [15] C.S. McGinnis, L.M. Murrow, and Z.J. Gartne. “DoubletFinder: dou-  
374 blet detection in single-cell RNA sequencing data using artificial nearest  
375 neighbors.” In: Cell systems 8.4 (2019), 329–337. e4.

376 [16] N.M. Xi and J.J. Li. “Benchmarking Computational Doublet-Detection  
377 Methods for Single-Cell RNA Sequencing Data”. In: Cell Systems 12.2  
378 (2021), 176–194.e6.

379 [17] D. J. McCarthy, K. R. Campbell, A. T. L. Lun, and Q. F. Wills.  
380 “Scater: pre-processing, quality control, normalization and visualiza-  
381 tion of single-cell RNA-seq data in R”. In: Bioinformatics 33.8 (Jan.  
382 2017), pp. 1179–1186. eprint: <https://academic.oup.com/bioinformatics/article-pdf/33/8/1179/25150420/btw777.pdf>.  
383

384 [18] J. Breda, M. Zavolan, and E. van Nimwegen. “Bayesian inference of  
385 gene expression states from single-cell RNA-seq data”. In: Nat Biotechnol  
386 (2021).

387 [19] V. D. Blondel, J.-L. Guillaume, R Lambiotte, and E. Lefebvre. “Fast  
388 unfolding of communities in large networks”. In: J. Stat. Mech. P10008  
389 (2008), p. 12.

390 [20] Peter J. Rousseeuw. “Silhouettes: A graphical aid to the interpretation  
391 and validation of cluster analysis”. In: Journal of Computational and Applied Mathematics  
392 20 (1987), pp. 53–65.

393 [21] L. Van der Maaten and G. Hinton. “Visualizing data using t-SNE”. In:  
394 Journal of Machine Learning Research 9 (2008), pp. 2579–2605.

395 [22] L. McInnes, J. Healy, N. Saul, and L. Großberger. “UMAP: uniform  
396 manifold approximation and projection”. In: J. Open Source Softw 3  
397 (2018), p. 861.

398 **10 Figures caption**

399 Figure 1 : A metromap view of the scAN10 pipeline.

400 Figure 2 : A. Number of detected genes when using different versions of the  
401 GTF file. B. Violin plot representation of the impact of the GTF version on  
402 the UMI counts for the CHGA gene.

403 Figure 3 : A. Number of detected genes when using either an unfiltered (106)  
404 of filtered (filter106) version of the GTF file. B. Violin plot representation of  
405 the filtration impact on the UMI counts for the CD68 gene.

406 Figure 4 : A. Number of detected genes when using either Cellranger (CR)  
407 or Kallisto-bustools (KB) as an alignment tool. B. Violin plot representation  
408 on the UMI counts for two genes, CHGA and RBP4.

409 Figure 5 : UMAP representation (A and B) and Silhouette scores (C and  
410 D) of the clusters obtained on data processed with CellRanger (A and C)  
411 or Kallisto-bustools (B and D). In E is shown an alluvial plot highlighting  
412 the conservation and differences in cluster composition depending upon the  
413 initial mapping method.

414 11 Figures

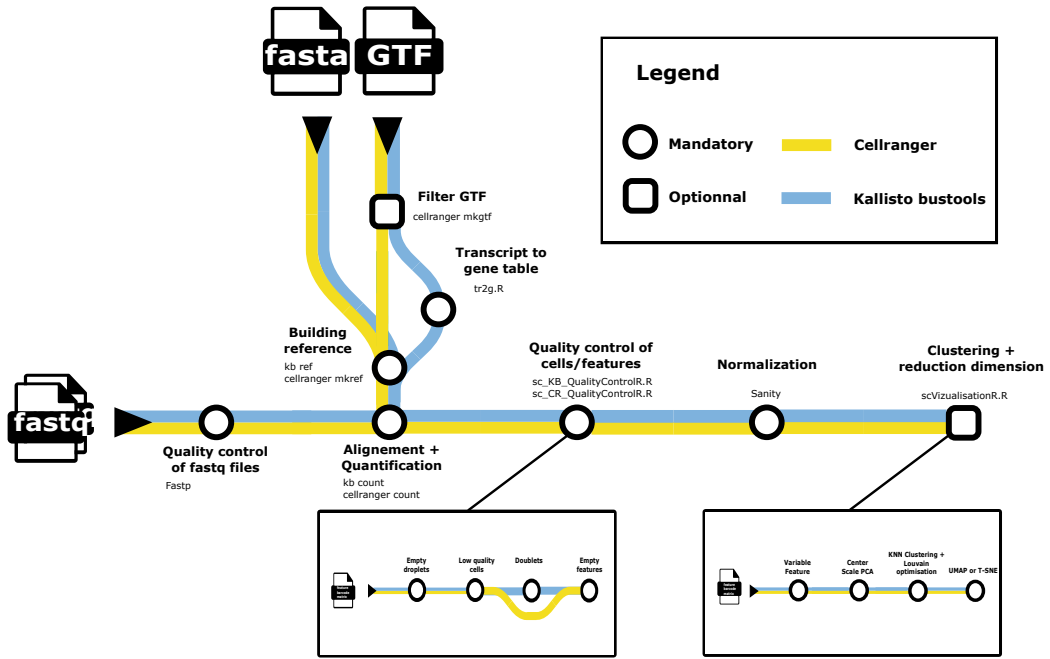


Figure 1

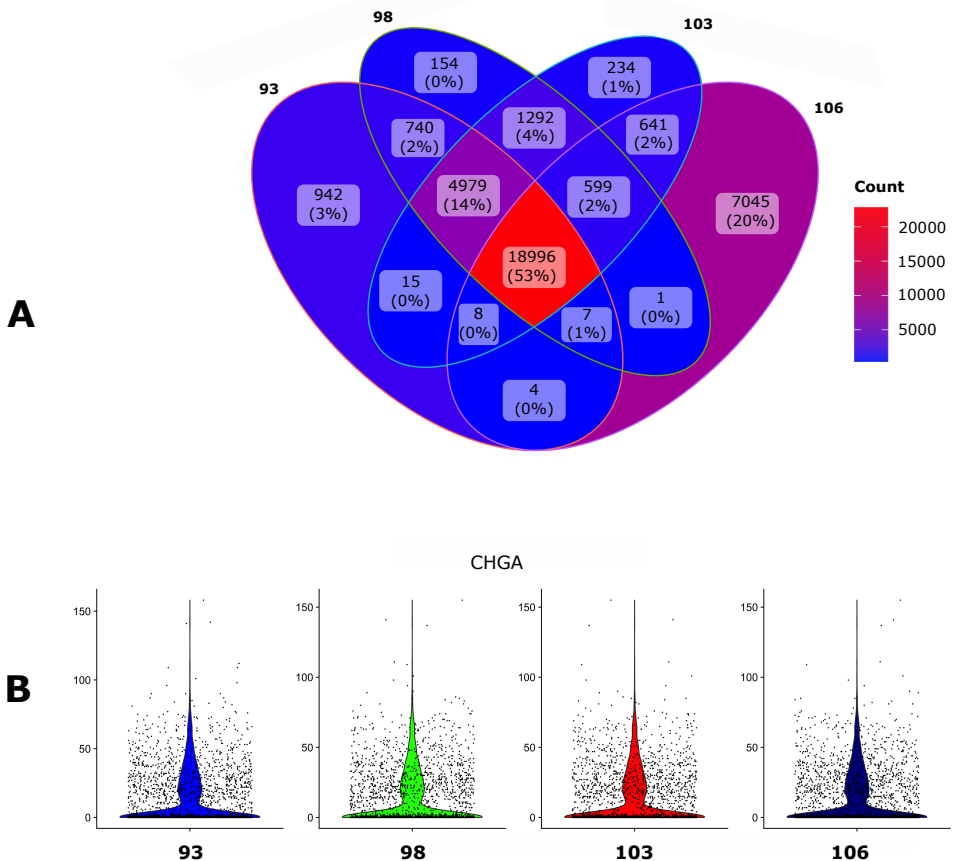
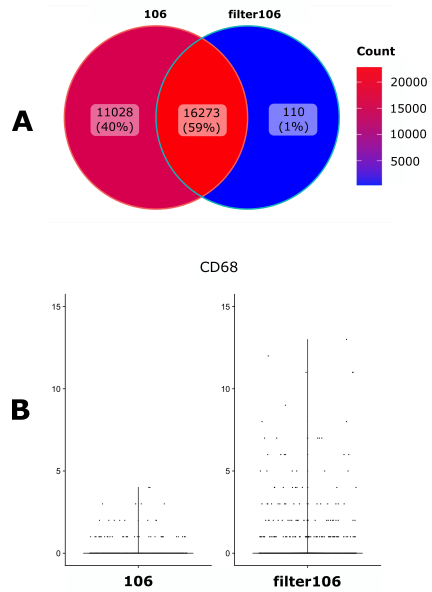


Figure 2



**Figure 3**

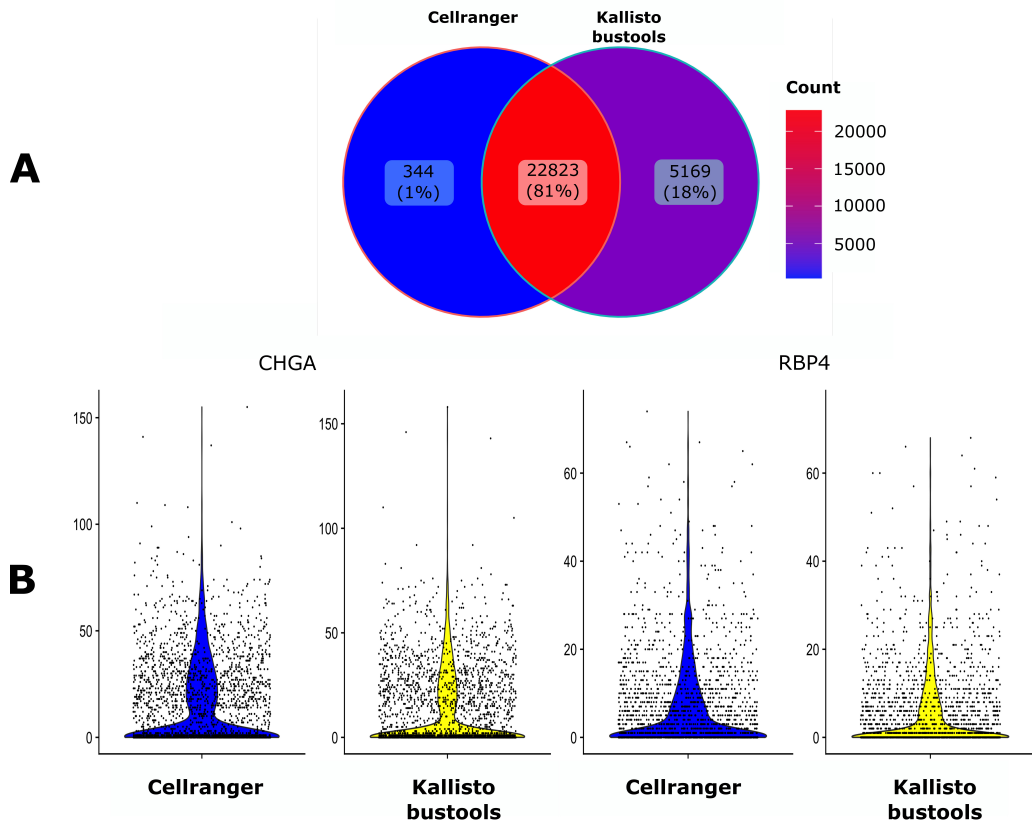
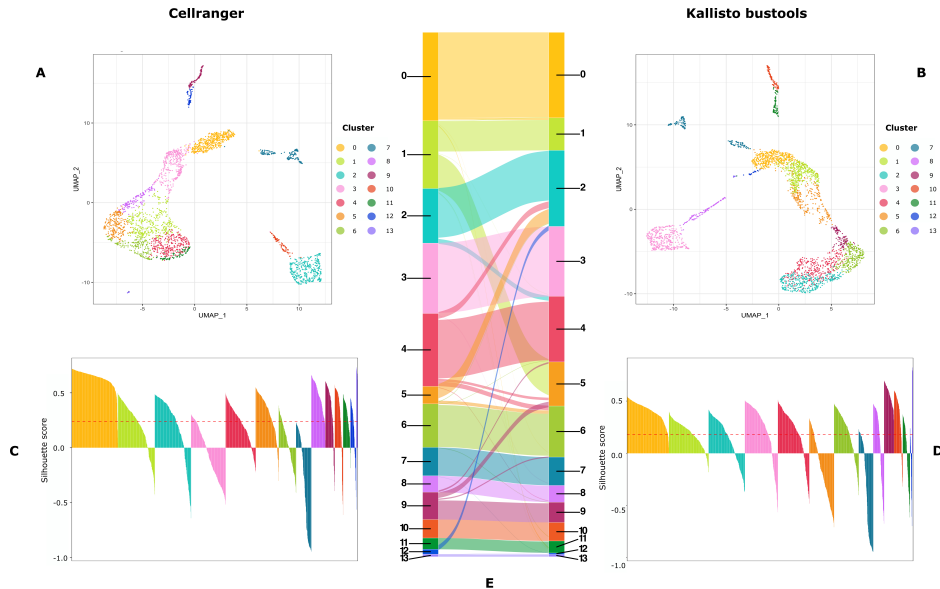


Figure 4



**Figure 5**